PEDIATRIC CRANIAL DEFECT SURFACE ANALYSIS FOR CRANIOSYNOSTOSIS POSTOPERATION CT IMAGES

Chia-Chi Teng[1], Linda G. Shapiro[2], Richard A. Hopper[3], Jon Ver Halen[3]

[1] School of Technology, Brigham Young University
[2] Department of Computer Science & Engineering, [3] Department of Surgery, University of Washington

ABSTRACT

Craniosynostosis is a congenital disease which consists of premature fusion of one or more cranial sutures, resulting in an abnormal head shape. Patients are usually treated by cranial vault expansion surgery to minimize the potential for brain damage. Full thickness cranial defects result from the expansion surgery, with the size directly proportional to the degree of expansion. The growing cranial skeleton has a unique regenerative capacity to heal small defects; however, when this regenerative capacity is exceeded, the defect is classed as one of critical size and requires surgical treatment to restore protection to the underlying brain. Although what constitutes a critical cranial defect is well known in animal models, it is not as clear for pediatric human skulls. The purpose of this study is to investigate a method that can effectively quantify healing of the pediatric cranial defect surface after cranial vault expansion surgery for craniosynostosis.

Index Terms – Biomedical imaging, Craniofacial

1. INTRODUCTION

Craniosynostosis is the pathological condition of early fusion of one or more of the growing sutures of an infant's skull, affecting 1 in 2,500 individuals. Normally, an infant is born with open sutures, allowing for the development and expansion of the brain (Fig. 1a). However, in children with craniosynostosis, one or more of these sutures close prematurely. The early closure of these sutures results in progressive deformity in calvarial shape due to the combination of restriction of osseous growth perpendicular to the fused suture and compensatory growth in unfused calvarial bone plates. Isolated sagittal synostosis, denoted by a long narrow skull shape (Fig. 1b) is the most common form of isolated suture synostosis with an incidence of approximately 1 in 5,000, accounting for 40-60% of single suture synostosis [1].

Craniofacial reconstructive surgery is usually required in the first year of life for pediatric patients with one or more sutures that have fused prematurely. Cranial defects are

(a) (b) (c)

Fig. 1. Three-dimensional reformations from CT imaging showing the top-view of a patient with a) a normal skull shape; b) a malformed skull affected with sagittal synostosis; the sagittal suture is completely absent; and c) a skull after a reconstructive surgery to restore intracranial volume.

common sequelae of such pediatric cranial surgery, as shown in Figure 1c. Animal models of critically-sized or non-healing cranial defects have been well-established [2]. For humans, we know that adult cranial defects do not heal spontaneously. The adult cranial skeleton demonstrates an inability to heal defects secondarily; thus, any clinically significant defect is a critical defect. While a child's growing cranial skeleton has a unique regenerative capacity to heal small defects, when this regenerative capacity is exceeded, the defect is classed as one of critical size and requires surgical treatment to restore protection to the underlying brain. We have little understanding of what constitutes a critical defect in children. In craniosynostosis surgery, it is particularly important to anticipate which defects will require additional intervention to close.

The purpose of this study was to investigate methods that can effectively measure the cranial defect surface from patients' CT images, which can in turn facilitate a quantitative study on the healing of cranial defects after craniosynostosis surgery.

2. BACKGROUND RESEARCH

Studies have been conducted to address the question of how post-pediatric cranial surgery defects heal [1] [2]. Although large retrospective case series reports have reported the ability for children to heal large calvarial defects, no quantitative study has been done. One of the reasons is that

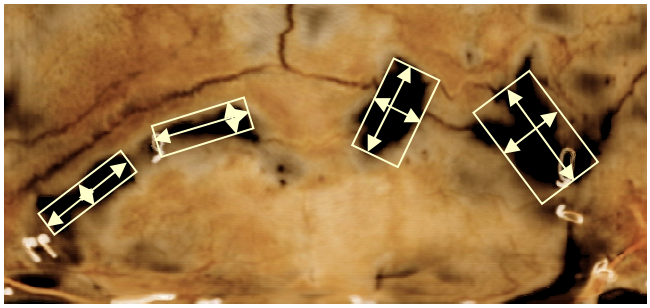

Fig. 2: Cranial defect surface estimation on 2D flattened skull image.

medical imaging techniques have not been widely applied to this particular field of study. No method has been developed to measure the size of the irregularly shaped three dimensional surface void of the skull from medical images.

Ver Halen et al [6] reviewed an existing database of CT scans of pediatric fronto-orbital advancement patients immediately postoperation (PO) and two years later (2Y). A quantitative comparison between the PO and 2Y cranial defects was conducted, but the defect surface areas were only estimated by the extents of the defect on two dimensional flattened coronal ring images of the skull as shown in Figure 2.

3. SYSTEM OVERVIEW

In our work, CT scans were performed postoperation (PO) and two years later (2Y) on all patients undergoing fronto-orbital advancement in this study. Each of the PO and 2Y three dimensional CT image sets is segmented to extract the 3D skull surface mesh. The skull base plane is defined by

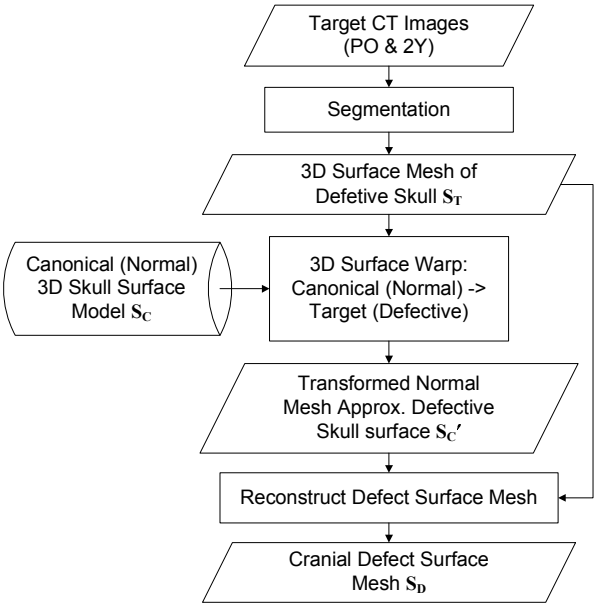

Fig. 3: System components block diagram.

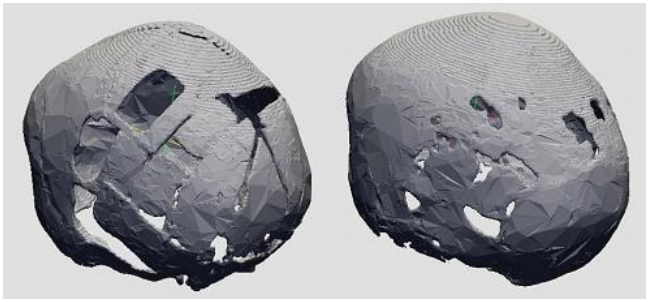

(a) (b)

Fig. 4: Fronto-orbital advancement patient skull surface mesh: a) postoperation; b) two year later.

(a) (b) (c)

Fig. 5: Surface warping: a) canonical surface mesh; b) transformed canonical model; c) target surface mesh.

using the frontal nasal suture anteriorly and opsithion posteriorly. The objective is to build 3D surface meshes that fill up the irregularly shaped defects and approximate a normal skull. The surface area of the meshes can then be used as a measurement for the defect area.

A canonical 3D skull surface model was obtained by segmenting a normal subject's CT images. A 3D surface warping algorithm [5] was used to transform the canonical skull surface $\mathbf{S_C}$ to be in alignment with the target subject's skull urface $\mathbf{S_T}$. The following energy function, for which smaller values indicate better alignment, is defined to evaluate possible correspondence relations:

$$E(C) = E_{sim}(C) + \alpha E_{str}(C) + \beta E_{pri}(C) \qquad (1)$$

where $\boldsymbol{C}$ is the function that maps points on surface $\mathbf{S_C}$ to matching points on surface $\mathbf{S_T}$, α and β are weight parameters, $\boldsymbol{E}_{sim}$ is the similarity term that measures how closely points on $\boldsymbol{C}(\mathbf{S_C})$ match points on $\mathbf{S_T}$, $\boldsymbol{E}_{str}$ is the structural term that minimize the distortion of surface $\mathbf{S_C}$, and $\boldsymbol{E}_{pri}$ is the "prior information" term, which ensures that $\boldsymbol{C}$ represent a plausible deformation. By minimizing the energy function $\boldsymbol{E}(\boldsymbol{C})$, we can bring $\boldsymbol{C}(\mathbf{S_C})$ in alignment with the target skull surface $\mathbf{S_T}$. This transformed canonical surface is defined as

$$\mathbf{S_C}' = \boldsymbol{C}(\mathbf{S_C}) \qquad (2)$$

where C minimize the energy function $\boldsymbol{E}(\boldsymbol{C})$ in Equation 1. Figure 5 shows an example of the surface warping result.

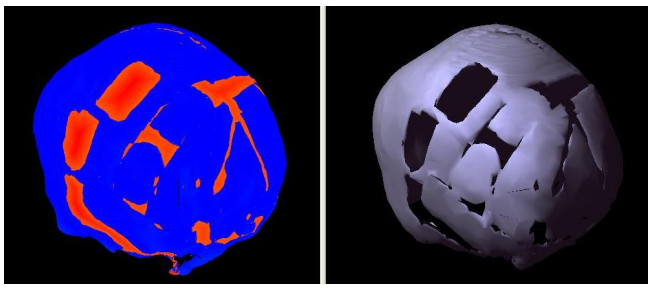

(a) (b)

Fig. 6: a) Sample points on the transformed canonical surface that corresponds to cranial defect area (in red); b) target surface.

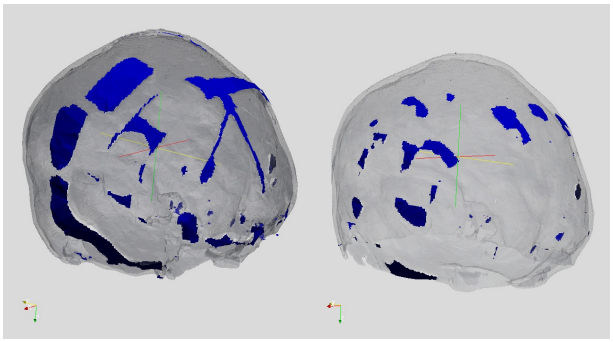

(a) (b)

Fig. 7: Cranial defect surface (in blue): a) postoperation; b) two year later.

From the two aligned surfaces $\mathbf{S_C}'$ and $\mathbf{S_T}$, we can reconstruct the surface mesh of the defect area. Figure 3 shows a simple block diagram illustrating the system components and the data flow.

4. RECONSTRUCTING DEFECT SURFACE

Let $\boldsymbol{P} = \{\mathbf{p}_i\}$ be a set of sufficiently dense sample points that lie on the transformed canonical surface $\mathbf{S_C}'$ approximating the target surface $\mathbf{S_T}$. The normalized surface normal at $\mathbf{p}_i$ is defined as $\mathbf{n}_i$. A ray $\boldsymbol{R_i}(t)$ with origin $\mathbf{p}_i$ and direction $\mathbf{n}_i$ is defined as

$$\boldsymbol{R_i}(t) = \mathbf{p}_i + t\,\mathbf{n}_i. \qquad (3)$$

The ray $\boldsymbol{R_i}(t)$ intersects the surface $\mathbf{S_T}$ at $t = t_i$, where $t_i = \infty$ if $\boldsymbol{R_i}$ does not intersect with $\mathbf{S_T}$. If $| t_i | <= \varepsilon$, then $\mathbf{p}_i$ corresponds to a non-defective location on surface $\mathbf{S_T}$. The value of ε is chosen to avoid $\boldsymbol{R_i}$ from intersecting with the surface of internal structure or on the opposite side of the skull. $\boldsymbol{P_D}$ is the subset of $\boldsymbol{P}$ that corresponds to cranial defect surface area as the following,

$$\boldsymbol{P_D} = \{\mathbf{p}_j\}, \text{ where } | t_i | > \varepsilon. \qquad (4)$$

Figure 6 shows an example of $\boldsymbol{P_D}$ on the transformed canonical (normal) surface $\mathbf{S_C}'$ that maps to the target (defective) surface $\mathbf{S_T}$.

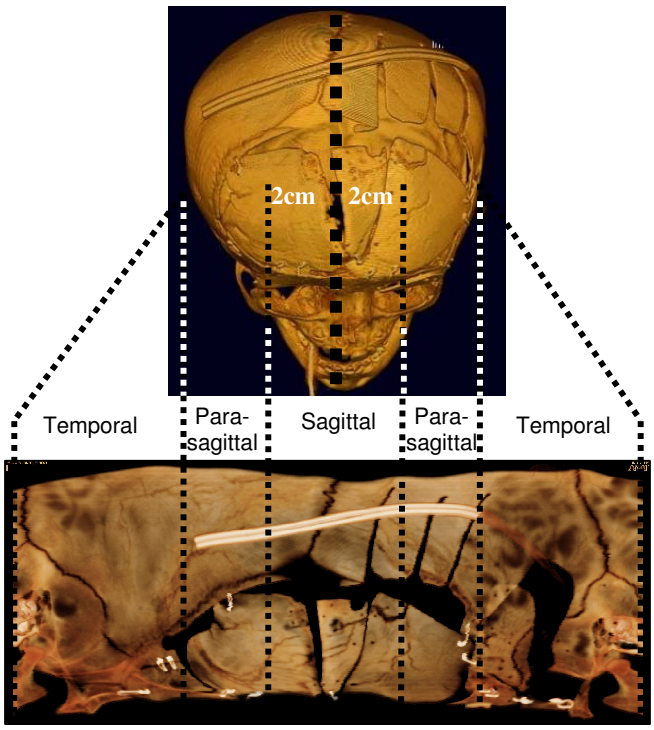

Fig. 8: Definition of cranial defect areas illustrated on flattened coronal ring.

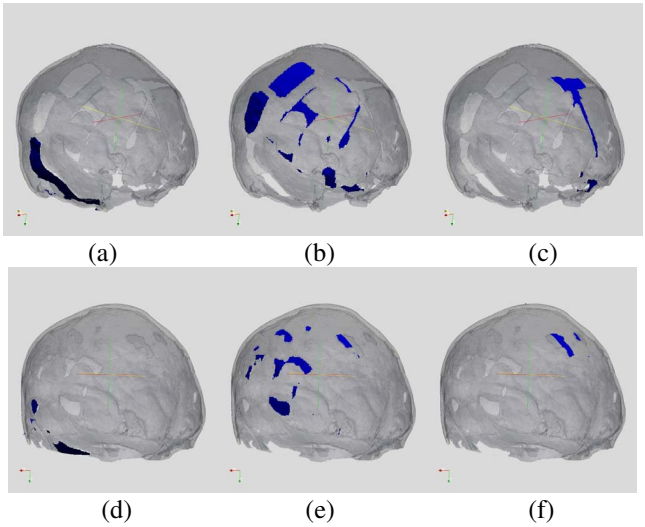

(a) (b) (c)

(d) (e) (f)

Fig. 9: Defect surface (in blue) divided into zones: a) PO left temporal; b) PO left para-sagittal; c) PO left sagittal; d) 2Y left temporal; e) 2Y left para-sagittal; f) 2Y left sagittal.

A surface mesh $\mathbf{S_D}$ which approximates the cranial defect area can be reconstructed from the point set $\boldsymbol{P_D}$ [7]. Figure 7 shows the resulting cranial defect surface for the craniosynostosis patient shown in Figure 4.

Once the surface mesh for the cranial defect area is obtained, the approximate surface area of the defect can be calculated by the sum of the area of all the triangular elements of the mesh. For example, the postoperation (PO)

TABLE I
FRACTIONAL HEALING COMPARISON BY ZONES

Defect Area by Zones (cm^2)	Left Temporal	Left Para-sagittal	Left Sagittal
Postoperation	9.12603	15.9472	4.99649
Two Year	2.95578	6.63699	1.4427
Fractional Healing	67.6%	58.4%	71.1%

cranial defect area (DA) measure in Figure 4(a) is 36.4 cm^2, and the two-year-later (2Y) DA in Figure 4(b) is 14.3 cm^2. The measurement of Fractional Healing [6] is defined as the following,

$$\mathbf{F} = [(\text{PODA} - 2\text{YDA})/\text{PODA}] \times 100\% \qquad (5)$$

where PODA is the postoperation defect area, and 2YDA is the 2-year-later defect area. The example above has the Fractional Healing of 60.7%.

Study [6] has shown that cranial defect heals differently depending on its location. It is important to quantitatively analyze the healing in different regions of the skull. Based on surgical relevance, for the purpose of this study, the cranial skeleton is divided into three paired zones: sagittal, parasagittal and temporal, as shown in Figure 8. We use ParaView [8] to cut the overall defect surface mesh into these zones. Figure 9 shows the defect surfaces in three zones on the left side of both the postoperation and the two-year-later example shown in Figure 7. With the defect surface divided into zones, we can calculate the Fractional Healing measures for each zone.

5. EXPERIMENT AND RESULTS

The CT scans were performed at Children's Hospital & Regional Medical Center in Seattle, Washington. At the time of this study, the database has 31 cases with complete protocol of postoperation and two-year-later CT images. The raw DICOM images were processed with ITK [9], which semi-automatically segments the skull and generates the triangular surface mesh.

It is worth noting that there are no published clinical or technical methods for quantitatively measuring the 3D cranial defect area. This is the first clinical application of its kind and there is no "ground truth" or "gold standard" for us to compare our results against. However, the results are verified by visual inspection to be reasonable approximation. We are also developing test cases (CT images) with artificial defects of known dimension as a calibrated control to verify the accuracy of the tool.

The proposed method can effectively build the cranial defect surface that approximate a normal skull and measure the area. It enables precise quantitative analysis for cranial defect healing in different regions. Increased understanding of the healing variables will help modify surgical techniques to minimize critical defects in pediatric craniosynostosis patients. As more engineered bone substitutes become available, this data will also help identify regions at high risk of non-healing and therefore appropriate for use of these materials. Table 1 shows a subset of Fractional Healing comparison for the patient shown in Figure 9.

6. CONCLUSION

The study of pediatric cranial defect healing will continue to improve the techniques and results of craniosynostosis surgery, and help indicate high-risk regions that would benefit from engineered bone substitutes. This work has provided a new and clinically relevant tool that can effectively measures the cranial defect area. As we continue to perform this surface analysis on all the CT scans in the growing database, we will be able to examine the effect of different craniosynostosis diagnoses and genetic mutations on defect healing.

There are many other potential applications for this work. For example, it can be used to study the three dimensional overlays of the defect surface from different points in time after the surgery, which could provide more information about different healing from the edges of the defect based on location and blood supply. It could also serve as a quality outcome measure by examining the 3D stability of the morphologic changes following cranial vault expansion by comparing immediate post-operative and two year later CT scans.

7. REFERENCES

[1] E. Lajeunie, M. Le Merrer, C. Marchac, D. Renier, "Genetic study of scaphocepaly". *American Journal Med. Gene.* 62, pp. 282-285, 1996.

[2] J.P. Schmitz, J.P. Hollinger, "The critical size defect as an experimental model for craniomandibulofacial nonunions." *Clin Ortho Rel Rsch* (205), pp. 299-308, 1986.

[3] M. Prevot, D. Renier, D. Marchac, "Lack of ossification after cranioplasty for craniosynostosis: A review of relevant factors in 592 consecutive patients." *Journal Craniofacial Surgery* 4(4), pp. 247-256, 1993.

[4] K.T. Paige, S.J. Vega, et al, "Age-dependent closure of bony defects after frontal orbital advancement." *Plastic Reconstructive Surgery* 118 (4), pp. 977-84, 2006.

[5] C.R. Shelton, "Morphable Surface Models," *International Journal of Computer Vision*, vol. 38, pp. 75-91, 2000.

[6] J. Ver Halen, R. Hopper, M. Cunningham, C. Birgfeld, J. Gruss, "Fractional Healing of Pediatric Coronal Ring Defects Two Years Following Fronto-Orbital Advancement for Craniosynostosis", *American Association of Plastic Surgeons Annual Meeting*, May 2007.

[7] H. Hoppe, T. DeRose, T. Duchamp, J. McDonald, W. Stuetzle. "Surface reconstruction from unorganized points". *SIGGRAPH 1992*, pp. 71-78.

[8] http://www.paraview.org

[9] http://www.itk.org